

Various scenarios for transition to thorium fuel cycle in the Single-fluid Double-zone Thorium Molten Salt Reactor (SD-TMSR)

O. Ashraf^{a,b,*}, Andrei Rykhlevskii^c, G. V. Tikhomirov^a, Kathryn D. Huff^c

^a*Laboratory of Engineering Computer Modeling in Nuclear Technologies, Institute of Nuclear Physics and Engineering, National Research Nuclear University MEPhI, Moscow, Russia, 115409*

^b*Physics Department, Faculty of Education, Ain Shams University, Cairo, Egypt, 11341*

^c*Dept. of Nuclear, Plasma, and Radiological Engineering, University of Illinois at Urbana-Champaign, Urbana, IL 61801, United States*

Abstract

Liquid-fueled Molten Salt Reactor (MSR) systems represent advances in safety, economics, sustainability, and proliferation-resistance. The MSR has been designed to operate in Th/²³³U fuel cycle with ²³³U used as start-up fissile material. Since ²³³U does not exist in nature, it is required to examine other available fissile materials. This work investigated the fuel cycle and neutronics performance of the Single-fluid Double-zone Thorium-based Molten Salt Reactor (SD-TMSR) with different fissile material loadings at start-up: Low-enriched uranium (LEU) (19.79%), Pu mixed with LEU (19.79%), Pu reactor-grade (a mixture of plutonium isotopes chemically extracted from Pressurized Water Reactor (PWR) spent fuel with 33 *GWd/tHM* burnup), Transuranic elements (TRU) from Light Water Reactor (LWR) spent nuclear fuel (SNF) and finally ²³³U. The MSR burnup routine provided by SERPENT-2 has been used to simulate the online reprocessing and refueling in the SD-TMSR. The effective multiplication factor, fuel salt composition evolution and net production of ²³³U have been studied in the present work. The results show that the continuous flow of Pu reactor-grade helps in transition to thorium fuel cycle within a relatively

*Corresponding Author

Email address: osama.ashraf@edu.asu.edu.eg oabdelaziz@mephi.ru (O. Ashraf)

short time (≈ 4.5 years) compared to 26 years for ^{233}U start-up fuel. Finally, using TRU as initial fissile materials shows the possibility of operating the SD-TMSR for a long period of time (≈ 40 years) without any external feed of ^{233}U .

Keywords: MSR, thorium fuel cycle, transmuter, burner, online reprocessing, Monte carlo code

1. Introduction

The Generation IV International Forum (GIF) has defined eight technology goals for the next generation nuclear systems. These goals have been defined in four broad areas: safety and reliability, economics, sustainability, non-proliferation and physical protection [1]. The Molten Salt Reactor (MSR) has many advantages that consistent with GIF's goals, for example, liquid fuel, inherent safety, online reprocessing and refueling, excellent neutron economy and operation near atmospheric pressure in a primary loop [2, 3]. Thus, the GIF selected MSR as one of the promising Generation-IV reactors [1, 4]. In the MSR, the fuel is dissolved in a molten salt (e.g., LiF or NaCl). This liquid fuel salt (e.g., LiF-BeF₂-ThF₄- ^{233}U F₄) constantly circulates through the core and allows transferring fission heat from reactor core to heat exchanger.

The Single-fluid Double-zone Thorium-based Molten Salt Reactor (SD-TMSR-2,250 MW_{th}) was introduced by the Chinese Academy of Sciences (CAS) [5]. The SD-TMSR is a graphite-moderated thermal-spectrum MSR operating in Th/ ^{233}U fuel cycle. In the SD-TMSR the fissile and fertile elements are integrated into the same salt. In addition, the active core is divided into two zones, the radius of the fuel channels in the outer zone is modified to be larger than the radius of the fuel channels in the inner zone to improve the breeding ratio [6, 5].

Historically, the thermal-spectrum MSR was designed for the Th/ ^{233}U fuel cycle [7, 6, 8, 3]. This design assumes that we have fissile ^{233}U inventory to startup new MSRs. But ^{233}U does not exist in the Earth's crust and can be produced from fertile ^{232}Th only in the nuclear reactor. Therefore, it is required

to examine alternative fissile materials (e.g., ^{235}U) to replace the ^{233}U in the
 25 startup fuel composition [9, 10]. The thorium fuel cycle transition can be achieved
 after reaching the doubling time¹ of ^{233}U because in this case all startup fissile
 material is being substituted by newly produced ^{233}U .

Betzler *et al.* discussed the simulation of the startup of a MSBR unit cell
 with Low-enriched uranium (LEU) (19.79%) and Pu from Light Water Reactor
 30 (LWR) spent fuel (SF) as initial fissile materials [9]. They concluded that the
 plutonium vector extracted from LWR SF is the best alternative source to ^{233}U
 because it has the highest ratio of fissile isotopes [9]. Zou *et al.* introduced two
 approaches for the thorium fuel cycle transition in Thorium-based Molten Salt
 Reactor (TMSR): (1) in-core transition and (2) ex-core transition. In the first
 35 approach, the TMSR is launched with existing fissile material and thorium as a
 fertile material; then the ^{233}U bred from thorium is rerouted into the core to
 maintain criticality. In contrast, the second approach tends to store produced
 ^{233}U out of the core until there is enough amount to start a new TMSR [10].
 Additionally, Zou *et al.* studied the transitioning to thorium fuel cycle in a small
 40 modular Th-based molten salt reactor (smTMSR) using Transuranic elements
 (TRU) as startup fuel. They concluded that the transition to thorium fuel cycle
 can be achieved in thermal smTMSR with a proper fuel fraction [11].

Heuer *et al.* discussed the transition characteristics of the Molten Salt Fast
 Reactor (MSFR) under different launching scenarios (e.g., enriched uranium
 45 and TRU) they concluded that starting the Thorium fuel cycle is feasible while
 closing the current fuel cycle and adopting stockpile incineration in MSRs for
 optimizing the long-term waste management [12].

Indeed, there are various researches that revolve around starting the MSRs
 with fissile materials alternative to ^{233}U . Many of these researches focus on
 50 the fast-spectrum MSRs [13, 14, 17, 18, 12, 15], while little focus on thermal-
 spectrum MSRs [9, 11, 10]. Nevertheless, starting the Single-fluid Double-zone
 Thorium-based Molten Salt Reactor (SD-TMSR) specifically with other fissile

¹Time required to produce enough amount of ^{233}U to trigger a new SD-TMSR.

materials (except ^{233}U) was not studied before. Therefore, the main object of the present paper is to discuss the simulation of the SD-TMSR operation for a lifetime-long period of time (60 years) with different initial fissile materials and without any external feed of ^{233}U to achieve the thorium fuel cycle transition. We investigated five different initial fissile materials: LEU, Pu mixed with LEU, Pu reactor-grade, TRU from LWR SF and ^{233}U [16]. Moreover, two different feed scenarios were selected:

- Continuous feed flow of thorium from Th stockpile and ^{233}U from **Pa-decay tank**², where the removal rate of ^{233}Pa = feed rate of ^{233}U . [9].
- Continuous injection of Heavy Metal (HM) (excluding Th) and simultaneously feed of all or part of produced ^{233}U from **Pa-decay tank**.

All calculations presented in the present paper were performed using SERPENT-2 version 2.1.30. We used the MSR burnup routine provided by SERPENT-2 to simulate continuous online reprocessing and refueling. SERPENT-2 uses an internal calculation routine for solving the set of Bateman equations describing the changes in the material compositions caused by neutron-induced reactions and radioactive decay [19]. Additionally, SERPENT-2 allows us to conduct the burnup calculations on computer clusters with multiple cores using distributed-memory MPI parallelization.

This present paper is organized as follows: after an introduction about MSR systems, the model description is discussed in section 2. Methodology and tools is described in section 3. Extraction and feed mechanisms are addressed in section 4. Section 5 focuses on the results and discussion. Finally, section 6 highlights the conclusions.

²An imaginary tank used to store protactinium extracted from the core.

2. Model description

2.1. Geometry

The SD-TMSR design model was introduced by the CAS as a part of the
80 strategic project “Future Advanced Nuclear Energy – Thorium-based Molten
Salt Reactor System (TMSR)” in 2011 [5, 20, 21, 22]. The design of SD-TMSR
is inspired by Molten Salt Breeder Reactor (MSBR) [23] after some modification
in the geometry to control the positive temperature coefficient in MSBR. The
SD-TMSR core geometry was described in details by Li *et al.* [5]. Figure 1
85 illustrates the quarter-core model configuration of the SD-TMSR. The active
zone is a right cylinder with height and diameter equal to 460 cm. Assemblies
of graphite³ hexagonal prisms fill the core. The side length of the graphite
hexagonal prism was optimized in [5] and found to be 7.5 cm. The liquid
fuel circulates continuously through the fuel channels that pierces the graphite
90 hexagonal prisms. The core is divided into two different zones to enhance
Th/²³³U breeding performance. The radius of the fuel channels in the outer and
inner zone are 5 and 3.5 cm, respectively. The axial and radial graphite reflectors
surround the core to minimize neutron leakage and maximize flux in the core.
The reflectors are surrounded by B₄C cylinder that acts as a radiation shielding.
95 The SD-TMSR pressure vessel holds the fuel salt, graphite elements, reflector,
shielding, intermediate heat exchanger (IHx) and made of Ni-based (hastelloy
N) alloy. The main characteristics of the SD-TMSR are listed in Table 1.

2.2. Fuel composition

The general composition of the liquid fuel salt in this work is 70LiF - 17.5BeF₂
100 - 12.5(HM)F₄ mole%, where HM is the heavy metal (mixture of thorium and
other actinides). The aim of this paper is to simulate the operation of SD-TMSR
for 60 years with different startup fissile compositions and without any external
feed of fissile ²³³U which we assumed is unavailable. For that reason, five different

³We choose graphite density of 2.3 g/cm³, to validate our results against results in the
literature [5, 6].

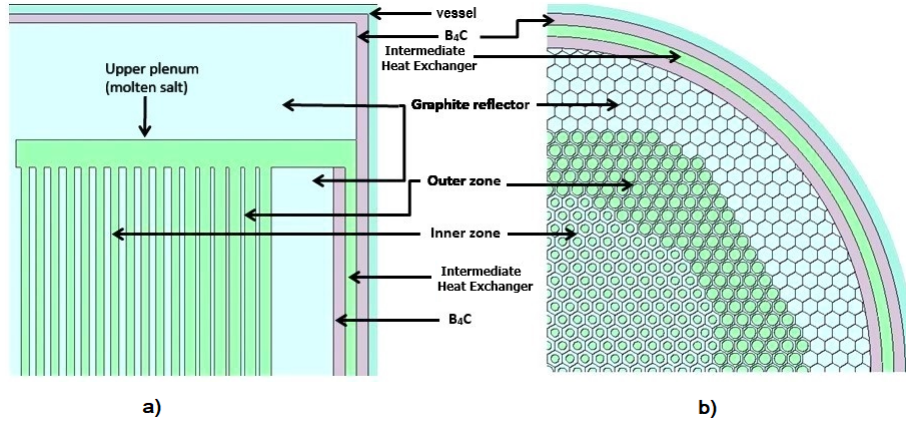


Figure 1: XZ (a) and XY (b) section of the quarter-core model of the SD-TMSR.

Table 1: The main characteristics of the SD-TMSR [5]

Thermal power, MW_{th}	2,250
Fuel salt components	LiF-BeF ₂ -(HM)F ₄
Fuel composition, mole%	70-17.5-12.5
⁷ Li enrichment, %	99.995
Fuel temperature, K	900
Fuel density at 900 K, g/cm ³	3.3
Fuel dilatation coefficient, g/(cm ³ .K)	-6.7×10^{-4}
Graphite density, g/cm ³	2.3
B ₄ C density, g/cm ³	2.52
¹⁰ B enrichment, %	18.4
Core diameter, cm	460
Core height, cm	460
Side length of the graphite hexagonal prism, cm	7.5
Inner radius, cm	3.5
Outer radius, cm	5
Ratio of molten salt and graphite in the inner zone	0.357
Ratio of molten salt and graphite in the outer zone	1.162
Fuel volume, m ³	52.9

Table 2: Reactor-grade plutonium vector (Mass fraction %) [24]

^{238}Pu	^{239}Pu	^{240}Pu	^{241}Pu	^{242}Pu
1.3	60.3	24.3	9.1	5

Table 3: TRU vector (Mass fraction %) [16]

^{237}Np	^{238}Pu	^{239}Pu	^{240}Pu	^{241}Pu	^{242}Pu	^{241}Am	^{243}Am	^{244}Cm	^{245}Cm
6.3	2.7	45.9	21.5	10.7	6.7	3.4	1.9	0.8	0.1

types of initial fissile materials based on LEU, Pu, and TRU from LWR SF were
105 considered:

- (a) low-enriched uranium (LEU) (19.79%);
- (b) Pu mixed with LEU (19.79%);
- (c) Pu reactor-grade [24];
- (d) transuranic (TRU) elements from LWR SF [16];
- 110 (e) ^{233}U for comparison purpose [25].

The reactor-grade plutonium and TRU composition are summarized in Table 2
and 3, respectively.

For reactor-grade plutonium case, the composition was taken for plutonium
recovered from the spent fuel composition of commercial Pressurized Water
115 Reactor (PWR) with the average discharge burnup 33 GWd/t and after 10 years
of cooling before reprocessing [26, 24]. Similarly, the isotopic compositions of
TRU was taken for the SF of UOX PWR (after one use, no multi-recycling)
with the average discharge 60 GWd/t burnup, and after 5 years of cooling [16].
The molar composition of startup fuel for all five cases is listed in Table 4.
120 Meanwhile, the corresponding initial nuclei inventories with different types of
fuel are summarized in Table 5.

Table 4: Composition of startup fuel (mole%)

Fuel component	salt	LEU (19.79%)	Pu+enriched U (19.79wt%)	Pu reactor- grade	TRU	²³³ U
LiF		70	70	70	70	70
BeF ₂		17.5	17.5	17.5	17.5	17.5
ThF ₄		8.25	7.5	10.75	8.65	12.3
UF ₄		4.25	4.75			0.2
PuF ₃			0.25	1.75		
(TRU)F ₃					3.85	

3. Methodology and tools

Simulation of Liquid-fueled Molten Salt Reactor (MSR) systems requires computational software that must support online fuel salt reprocessing and refueling [27]. In this work, SERPENT-2 version 2.1.31 beta⁴ [19] is used to simulate the full-core of the SD-TMSR with different types of initial fuel. The extension of SERPENT accounts for continuous online reprocessing and refueling [28]. ENDF-VII.0 cross-section library was used for all calculations in this work. The results demonstrate full-core runs of 1.25×10^7 neutron history per depletion step. The full burnup time of the SD-TMSR was 60 years with statistical error in k_{eff} equal to ± 36 pcm. The online extraction of Fission Products (FPs) and other neutron absorbers provides many benefits for MSRs. For example, it would reduce the initial fissile material inventory required to achieve criticality and improve the breeding ratio. Figure 2 shows a flow chart of the calculation steps.

As shown in Figure 2, after launched the input file, an advanced matrix exponential solution based on the Chebyshev Rational Approximation Method (CRAM) [29] used to solve the Bateman equation. Then, the system extracted gaseous FPs and other materials (non-dissolved metals, lanthanides, and soluble

⁴SERPENT-2 is a 3D continuous energy Monte Carlo neutron transport and burnup code.

Table 5: Initial nuclei inventories (in grams) of the SD-TMSR with different types of fuel.

Molecule	LEU (19.79%)	Pu mixed with en- riched U (19.79%)	Pu reactor- grade	TRU	²³³ U
²³² Th	6.24E+07	4.67E+07	6.75E+07	5.44E+07	7.69E+07
²³³ U					1.30E+06
²³⁵ U	3.17E+06	6.01E+06			
²³⁸ U	1.28E+07	2.43E+07			
²³⁷ Np				1.58E+06	
²³⁸ Pu		1.60E+04	1.13E+05	6.78E+05	
²³⁹ Pu		9.59E+05	6.76E+06	1.15E+07	
²⁴⁰ Pu		3.99E+05	2.82E+06	5.40E+06	
²⁴¹ Pu		1.60E+05	1.13E+06	2.69E+06	
²⁴² Pu		6.39E+04	4.51E+05	1.68E+06	
²⁴¹ Am				8.53E+05	
²⁴² Am					
²⁴³ Am				4.77E+05	
²⁴⁴ Cm				2.01E+05	
²⁴⁵ Cm				2.51E+04	
Total mass of HM without ²³² Th	1.60E+07	3.20E+07	1.13E+07	2.51E+07	1.30E+06

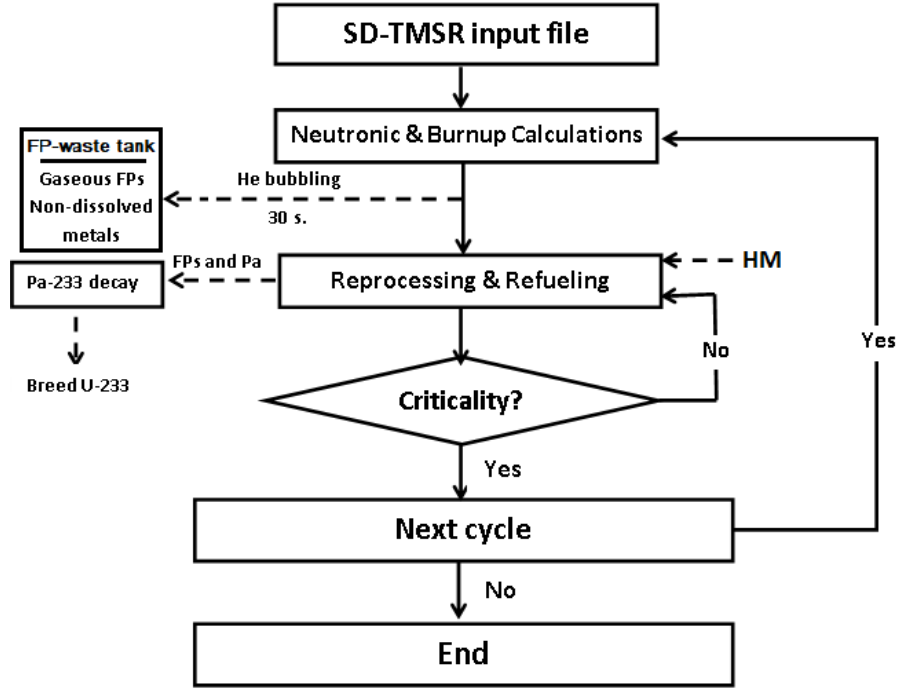


Figure 2: Flow chart of the calculation procedures.

metals except Pu) with suitable removal rate⁵. This can be done by set the flow rate of gaseous FPs and other materials from the fuel to the **FP-waste tank**⁶. Specifically, protactinium was removed from the fuel with a certain flow rate into the external tank, **pa-decay tank**, to decay and produce ^{233}U ⁷. The produced ^{233}U is used as a fresh fissile fuel and the residual ^{233}U is the net production of ^{233}U . The MSR burnup routine provided by SERPENT-2 allows changes the flow rates (*mflow*) of the isotopes during reactor operation [28]. Specifically, we have to determine the mass flow (*mflow*), which is the rate by which elements or nuclides are transferred between materials. After that, the transfer rates should be connected to materials with a reprocessing scheme. Finally, we have to link

⁵The extraction rate depends on the type of poison and its impact on the neutron economy.

⁶An imaginary tank used to store the gaseous FPs and the other materials (non-dissolved metals, lanthanides, and soluble metals except protactinium).

⁷The ^{233}Pa is removed and left to decay into ^{233}U with $\tau_{1/2} \approx 27 d$.

150 the reprocessing schemes to depletion histories. In the present work, we adjusted
the transfer rates of fresh fuel to maintain core criticality and to keep fuel salt
inventory constant during burnup. The feed constant calculation procedures are
summarized as follows:

1. The simulation started without any injection of refueling materials (i.e.
155 with only removing of FPs and Pa).
2. After first depletion calculation step, we checked the total mass density of
FPs and Pa in `FP-waste tank` and `pa-tank`, respectively.
3. A simple calculation yields the amount of Th and ^{233}U that must be added
during this cycle (mass of Th \approx mass of extracted FPs and mass of ^{233}U
160 \approx mass of extracted Pa).
4. Dividing this mass by time and inventory of refueling material gave the
corresponding feed constant.

The cycle calculation ran iteratively until the burnup reached the desired worth.

4. Feed and extraction rates

165 In the present work, two different feed mechanisms are used. The first
mechanism allows continuous feed flow of thorium from Th stockpile, and ^{233}U
from `pa-decay tank`. In contrast, the second mechanism continuously injects
Heavy Metal (HM) (excluding Th) and simultaneously feeds all or part of
produced ^{233}U from `Pa-decay tank`. The fission products act as poisons in
170 the MSRs; they negatively impacting the reactivity. Therefore, FPs must be
extracted during reactor operation. Consider T_r as the time during which the
total fuel salt is reprocessed and dN_e as the amount of particular element e with
inventory N_e that the MSR extracts during time dt ; thus [6]

$$\frac{dN_e}{dt} = N_e \frac{\varepsilon_e}{T_r}, \quad (1)$$

where ε_e is the removal efficiency. Equation 1 gives the removal constant λ_e [s^{-1}] (the rate at which the material is removed), where $\lambda_e = \varepsilon_e/T_r$. The removal constant λ_e of gaseous and other fission products is precisely calculated and summarized in Table 6. The effective reprocessing time for the gaseous FPs and non-dissolved metals was set to 30 seconds (removal constant $\lambda_e = -0.0333 s^{-1}$), because such elements must be extracted promptly and continuously via gas removal system. In contrast, extracting the soluble FPs, lanthanides, and protactinium can be done by the chemical reprocessing (i.e. fluorination and reduction reaction). Therefore, the system reprocesses a specific amount of fuel salt daily. In the present work, the effective extraction time for soluble FPs is ≈ 10.59 days ($\lambda_e = -1.092 \times 10^{-6} s^{-1}$), which is equivalent to $5 m^3/d$ of chemical reprocessing rate [6, 5]. The effective feed rates of the heavy metals (HM) are changed during reactor operation to conserve the total fuel mass and criticality.

Table 6: The reprocessing table.

Reprocessing group	Element	Reprocessing time	Removal constant λ_e [s^{-1}]
Gaseous FPs and non-dissolved metals	H, He, N, O, Ne, Ar, Kr, Nb, Mo, Tc, Ru, Rh, Pd, Ag, Sb, Te, Xe, Lu, Hf, Ta, W, Re, Os, Ir, Pt, Au and Rn.	30s	-3.333E-02
Lanthanides and other soluble FPs	Zn, Ga, Ge, As, Se, Br, Rb, Sr, Y, Zr, Cd, In, Sn, I, Cs, Ba, La, Ce, Pr, Nd, Pm, Sm, Eu, Gd, Tb, Dy, Ho, Er, Tm and Yb.	10.599 d ($5 m^3/d$)	-1.092E-06
Protactinium	Pa	10.599 d ($5 m^3/d$)	-1.092E-06

5. Results and discussion

5.1. Thorium feed mechanism

The first mechanism adopts continuous feed flow of external thorium and ²³³U from Pa-decay tank. Hereinafter the first mechanism will be mentioned as the thorium feed mechanism. The molar fraction of the heavy metal in the initial fuel was kept constant and equal to 12.5 mole% for all cases. Besides, the initial fissile material fraction was increased for the five fuel salt compositions until the SD-TMS reactor was sufficiently critical at the Beginning Of Life (BOL). Figure 3 illustrates the change of the effective multiplication with Effective Full-Power Years (EFPY) for the thorium feed mechanism. As shown in Figure 3, the effective multiplication factor (k_{eff}) decreases sharply during the first 25 years of reactor operation for the first four cases. k_{eff} decreases as a result of depletion of the initial fissile materials and generation of the neutron poisons (FPs). Thus, the reactor becomes subcritical within a relatively short time (≈ 4 years in the TRU case and ≈ 12 years in the Pu reactor-grade case). The amount of ²³³U generated in the SD-TMSR is not enough to conserve the reactor criticality and overcome the neutron absorption in the initial fertile isotopes. Nevertheless, the continuous feed flow of thorium and ²³³U helps to operate the SD-TMSR for a long period of time (the U-233 case). Additionally, the initial molar fraction in the LEU and Pu reactor-grade cases was increased more (see Figure 3) to counteract the absorption of neutrons in the non-fissile heavy metals added with the initial fuel salt. But k_{eff} still decreases below 1.0, as a result of increasing the non-fissile heavy metals in the initial fuel [9].

5.2. Non-thorium feed mechanism

The second mechanism allows continuous feed flow of ²³³U from Pa-decay tank and Heavy Metal except for Th. Hereinafter the second mechanism will be mentioned as the non-thorium feed mechanism. Figure 4 shows the change of the effective multiplication during 60 EFPY of reactor operation for the non-thorium feed mechanism. As shown in Figure 4, the SD-TMS reactor was

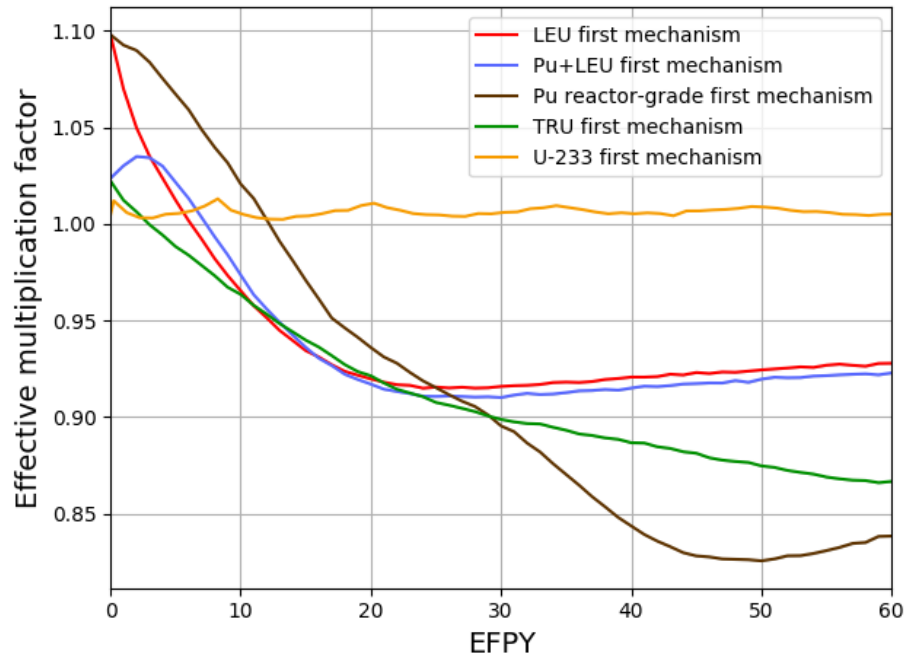


Figure 3: The change of the effective multiplication factor during 60 EFPY of reactor operation for thorium feed mechanism (confidence interval $\pm\sigma$ is shaded).

sufficiently critical at the Beginning Of Life (BOL). Both Pu reactor-grade and TRU case show promising results relative to the other two cases (i.e. LEU and Pu+LEU). For the Pu reactor-grade fuel salt, the amount of ^{233}U generated in the SD-TMSR in addition to the external feed flow of Pu are sufficient to
220 maintain the reactor criticality and overcome the neutron absorption in the initial non-fissile isotopes. This may be attributed to the fact that the spectrum in the Pu reactor-grade initial core is hardened that is more thorium is being converted to ^{233}U . For the TRU fuel salt, the amount of ^{233}U and the external feed flow of TRU is barely enough to operate the reactor for a long period of time
225 (≈ 40 years) without any external feed of ^{233}U . Nevertheless, k_{eff} decreases with the burnup because the Minor Actinides⁸ (MA) accumulating in the core as a result of continuous TRU feed. As shown in Figure 4, the LEU and Pu+LEU fuel are less attractive for non-thorium feed mechanism. The continuous LEU feed increases the amount of fertile ^{238}U and consequently, reduces the feasibility
230 of such fissile materials. The continuous feed of ^{233}U without ^{232}Th will lead to supercritical reactor, thus the ^{233}U case is excluded from non-thorium feed mechanism.

According to the k_{eff} results, Pu reactor-grade and TRU fissile materials are selected and discussed in the following.

235 5.3. Pu reactor-grade, TRU, and ^{233}U initial fuel

In this section, the simulation of the SD-TMSR with Pu reactor-grade and TRU fissile materials is discussed. Besides, the ^{233}U case is listed for comparison. Figure 5 demonstrates the dynamics of heavy metal refill rate during 60 EFPY of SD-TMSR operation. The heavy metal refill rate was adjusted to maintain;
240 the reactor criticality and total fuel mass almost constant⁹ during the reactor operation. In ^{233}U case, the mean values of ^{233}U and ^{232}Th refill rate are 1.77 and 2.21 kg/d, respectively. As well, in the Pu reactor-grade case, the mean

⁸In the present work, the Minor Actinides (MA) include Np, Am and Cm.

⁹The variation of the total fuel mass is less than 0.1%

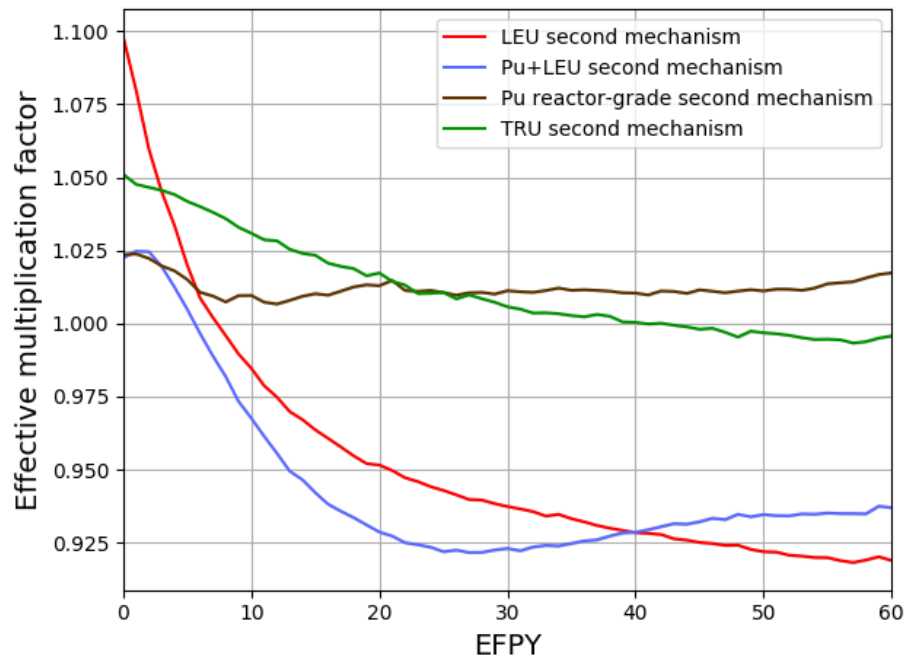


Figure 4: The change of the effective multiplication factor during 60 EFPY of reactor operation for non-thorium feed mechanism (confidence interval $\pm\sigma$ is shaded).

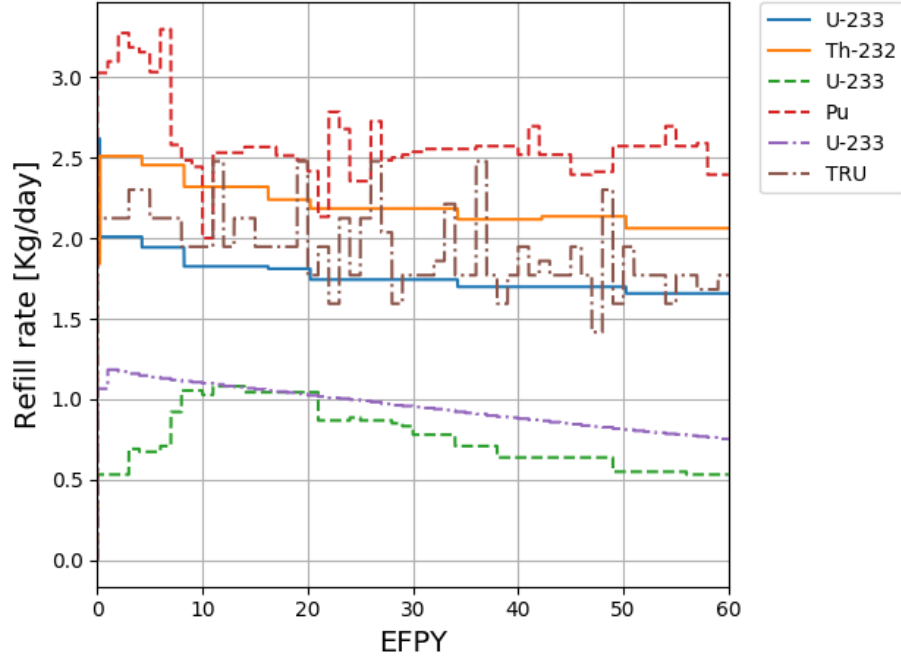


Figure 5: Dynamics of heavy metal refill rate during 60 EFPY of reactor operation. Solid lines for ^{233}U case, dashed lines for Pu reactor-grade case, and dotted lines for TRU case.

values of ^{233}U and Pu refill rate are 0.75 and 2.75 kg/d , respectively. In the TRU case, the mean values of ^{233}U and TRU refill rate are 0.90 and 2.0 kg/d , respectively.

Figure 6 and 7 describe the evolution of important isotopes for ^{233}U , Pu and TRU cases respectively. From Figure 6, the mass of Pa in the fuel salt is almost constant and reaches 17.8 kg at the end of the operation time. In addition, the mass of Minor Actinides (MA) increases with time; however, by applying online reprocessing, its value remains relatively low. As well, the total mass of Pu increases with burnup. The level of Pu in the fuel correlates with the mass of the MA, and Pu. MA need more time to reach equilibrium. The total mass of U increases with burnup and reaches equilibrium after ≈ 27 years. As shown in Figure 6, refueling the core with Th helps maintain an almost constant inventory throughout the full operation time.

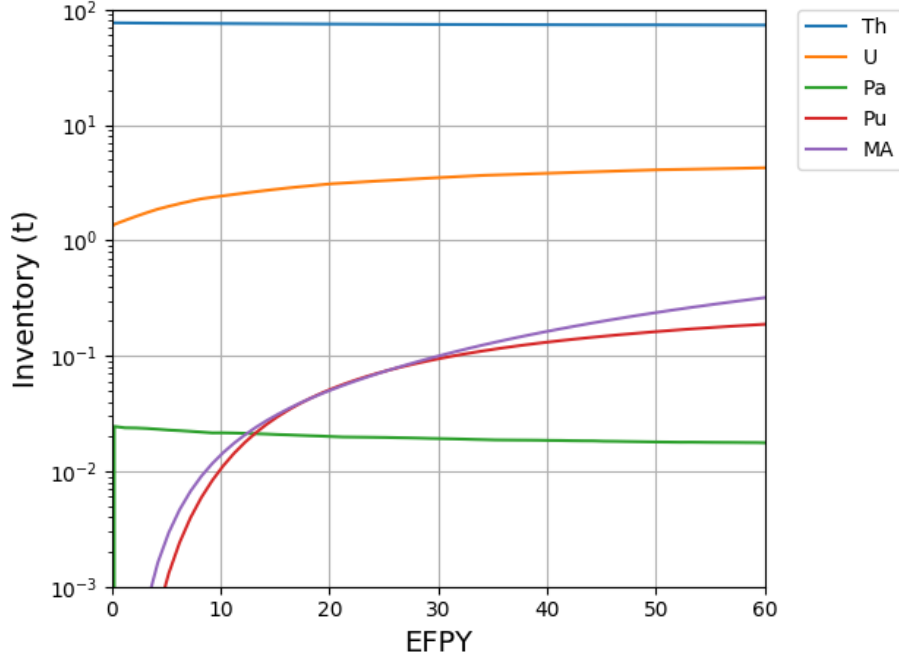


Figure 6: Evolution of the important nuclides inventories for ^{233}U case (MA involves Np, Am, Cm).

The Pa extraction time was adjusted to be 30 seconds for Pu and TRU cases to avoid poisoning the core. Therefore, Figure 7 shows that the mass of Pa in the fuel for Pu and TRU cases is relatively low when compared to the ^{233}U case. Major isotopes for the three cases reaches the equilibrium state after ≈ 30 years (see Figure 6 and 7).

Figure 8 illustrates the variation of thorium mass in the fuel salt for ^{233}U , Pu reactor-grade and TRU cases, respectively. In ^{233}U case, we apply the thorium feed mechanism, thus thorium mass decreases by only 3.2 % at the end of operation time (60 years). In contrast, thorium mass decreases significantly in Pu and TRU cases according to the non-thorium feed mechanism. Thorium mass decreases by 39.2 % and 37.96 % in Pu reactor-grade and TRU cases, respectively. The more decreasing in thorium mass, the more effective utilization of thorium fuel cycle. Consequently, the Pu reactor-grade initial fuel may help

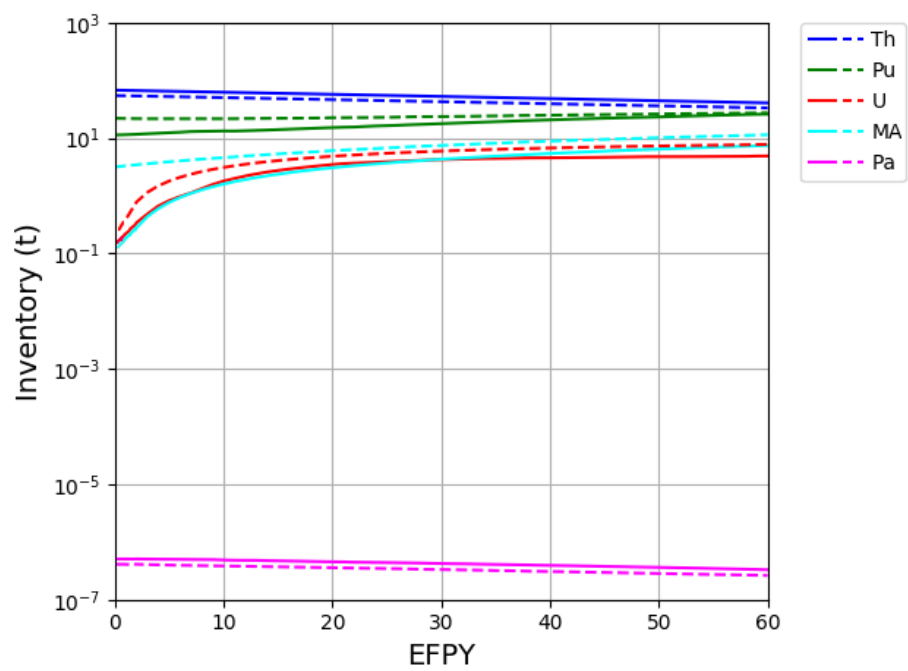


Figure 7: Evolution of the important nuclides inventories for Pu reactor-grade case (solid lines) and for TRU case (dashed lines).

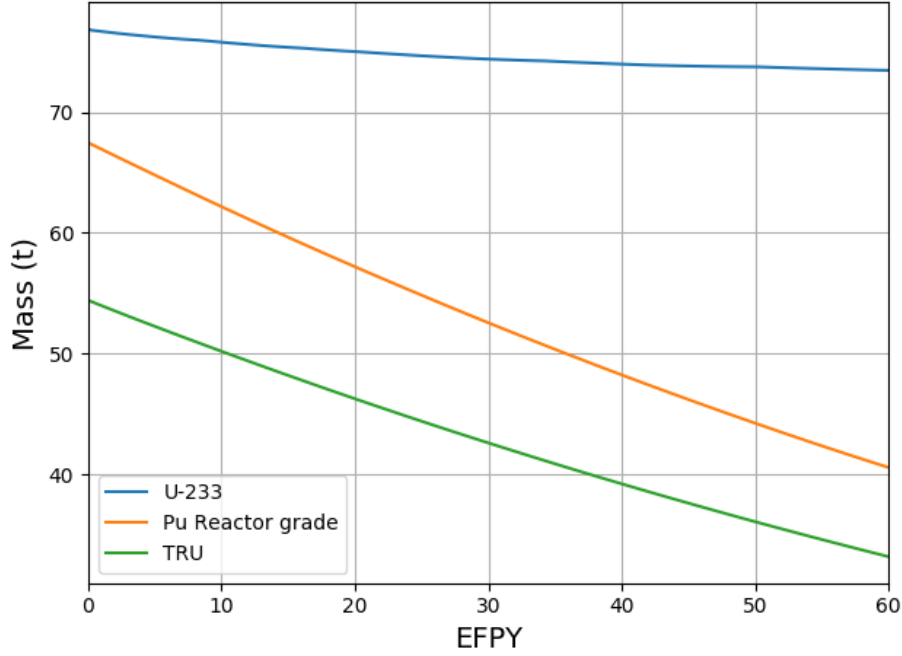


Figure 8: The variation of thorium mass in the fuel salt for ^{233}U , Pu reactor-grade and TRU cases, respectively.

to utilize thorium fuel cycle more effective.

Figure 9 demonstrates the mass of ^{233}U in the fuel salt for ^{233}U , Pu reactor-grade and TRU cases, respectively. One can see that the mass of the ^{233}U reaches the equilibrium state after ≈ 30 years. Meanwhile, the amount of ^{233}U is sufficient to maintain criticality in the three cases.

In the non-thorium feed mechanism, the SD-TMSR is continuously refueled for criticality, which increases the Pu proportion in the molten salt. According to the literature, the limit of Pu solubility in the FLiBe salt is $\approx 4.0\%$ [30, 31]. Figure 10 represents the Pu proportion in the fuel salt (mole%). In ^{233}U and Pu reactor-grade cases, the Pu proportion increases slightly but still below its solubility limit. On the other hand, the Pu proportion in the molten salt loaded by TRU increases with operation time and reaches the Pu solubility limit after ≈ 40 years. This issue may be solved by increasing the reactor operation

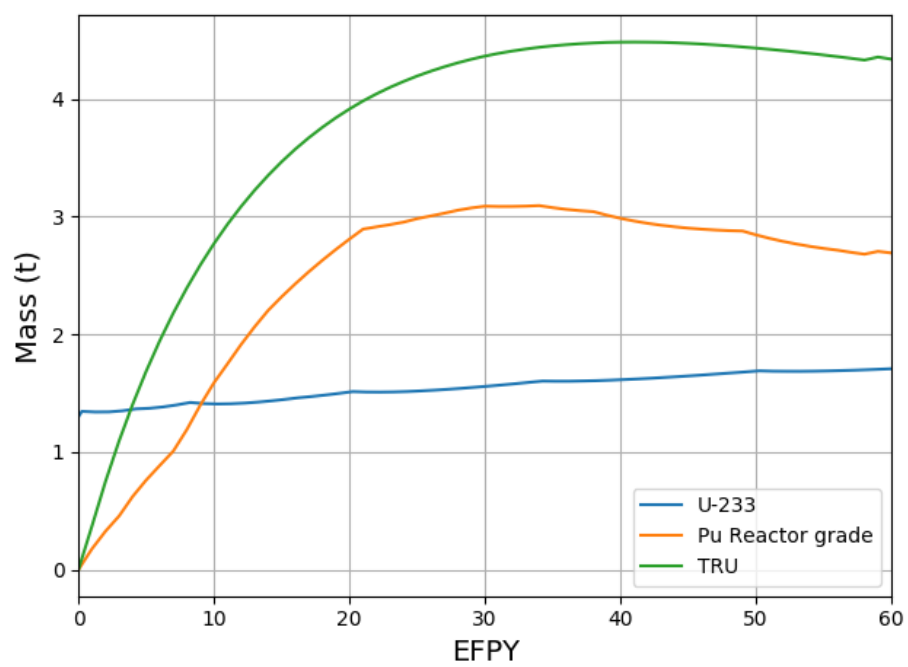


Figure 9: Mass of ^{233}U in the fuel salt for ^{233}U , Pu reactor-grade and TRU case, respectively.

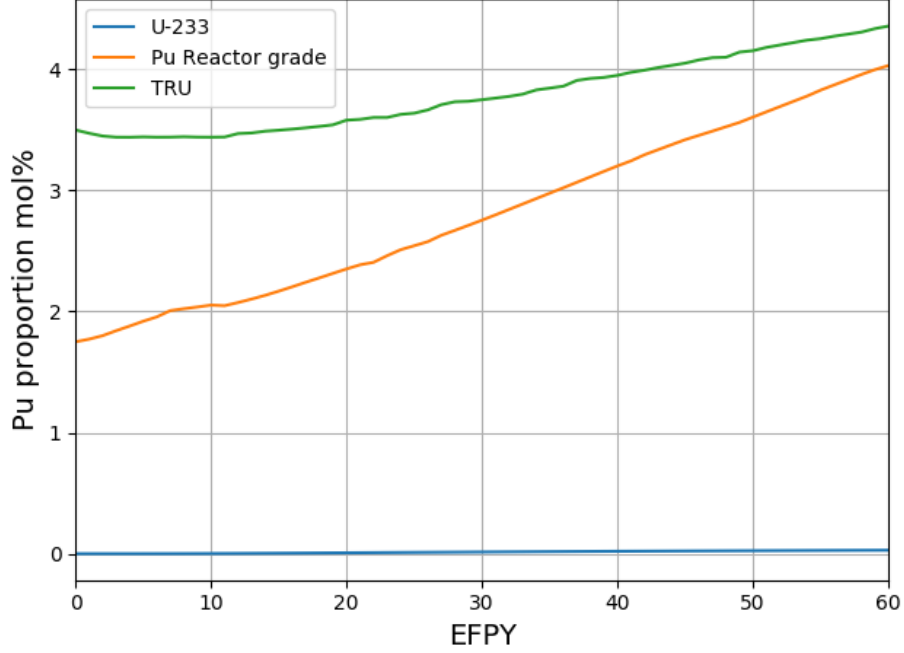


Figure 10: The Pu proportion in the fuel salt (mole%).

temperature and or reducing the HM initial inventory [10].

Figure 11 demonstrates the net production of ^{233}U as a function of burnup. In TRU case, the net production of ^{233}U is almost zero, nevertheless, the reactor becomes subcritical after 40 *years* of operation. In ^{233}U and Pu reactor-grade cases, the net production of ^{233}U increases with burnup and reaches about 1.77 *t* and 10 *t*, respectively at the end of operation lifetime. It worth noting that thorium feed mechanism is applied in ^{233}U case, while, non-thorium feed mechanism is adopted in Pu reactor-grade cases. As shown in Figure 11, after 26 *years* the net production of ^{233}U reaches 1.3 *t*; this is sufficient to start-up another SD-TMSR. Similarly, one can see that the same amount of ^{233}U (i.e. 1.3 *t*) can be achieved after ≈ 4.5 *years* if we applied the non-thorium feed mechanism on the SD-TMSR that initially loaded by Pu reactor-grade alternative to ^{233}U . In addition, Figure 11 also shows that the net production of ^{233}U during the first 455 days is negative, thus about 175.28 *kg* of ^{233}U must be added during

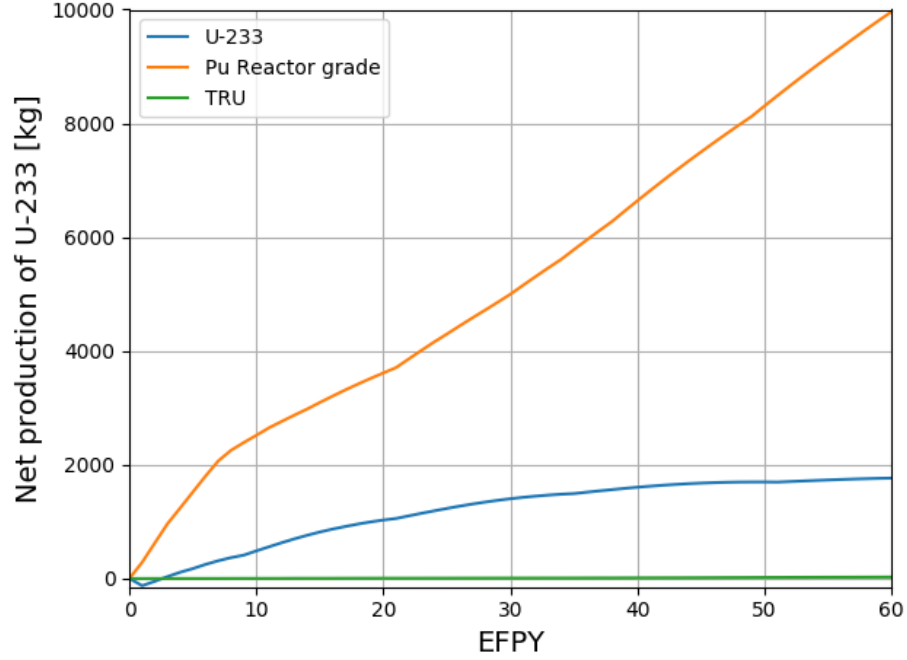


Figure 11: Net production of ^{233}U during burn-up period (60 EFPY).

this period. In conclusion, the thorium fuel cycle transition can be achieved by selecting the proper feed mechanism and initial fissile material.

5.4. Neutron spectrum

Figure 12 represents the neutron flux per unit lethargy for full-core SD-TMSR model in the energy range from 10^{-8} to 10 MeV for the ^{233}U , Pu reactor-grade, and TRU started case. In ^{233}U case, at the EOL, the neutron spectrum is harder than at BOL due to the accumulation of the Pu and other strong thermal neutron absorbers in the fuel salt. For Pu reactor-grade and TRU cases, during the reactor operation, the fissile Pu is depleted and the ^{233}U becomes the major fissile isotope (see Figure 9), the neutron spectrum softens and becomes similar to a thermal spectrum of the TMSR.

The comparison between the two feed mechanisms with different types of initial fuel is listed in Table 7.

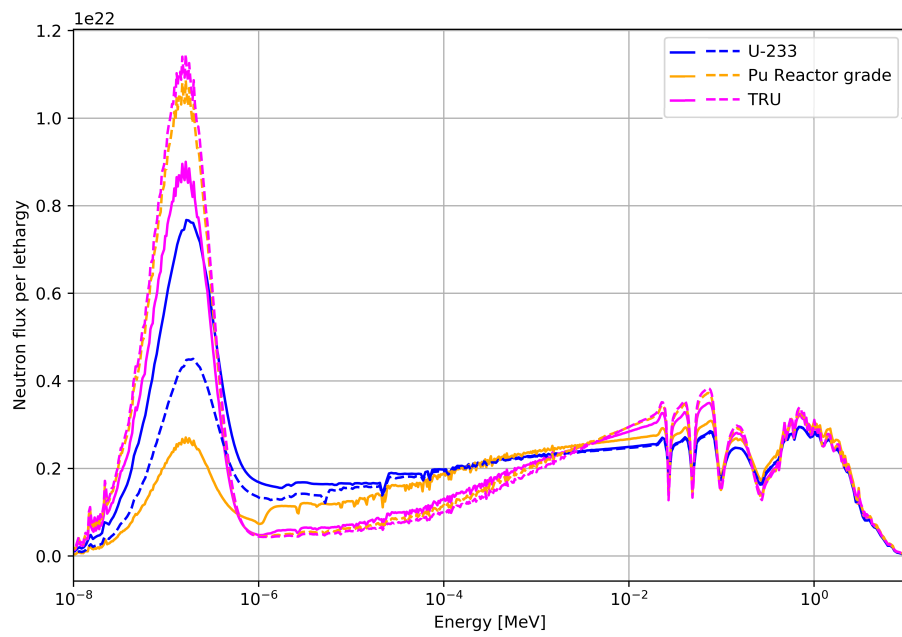


Figure 12: The neutron flux energy spectrum at BOL (solid lines) and EOL (dashed lines) for ^{233}U , Pu reactor-grade, and TRU case.

Table 7: Comparison between the two feed mechanisms for the five different types of initial fuel.

Feed mechanism	Initial fuel	LEU	Pu	Pu	TRU	^{233}U
		(19.79%)	mixed with enriched U (19.79 wt-%)	reactor-grade		
Thorium feed mechanism		Not work	Not work	Not work	Not work	Work
Non-thorium feed mechanism		Not work	Not work	Work well with positive net production of ^{233}U	Work for 40 <i>years</i> with net production of ^{233}U = zero	Not examined (super-critical reactor)

5.5. Neutron flux

Figures 13, 14 show the radial distribution of fast (energy range between 0.625 eV and 20 MeV) and thermal (energy range between 10^{-5} eV and 0.625 eV) neutron flux for three different initial fissile materials in the fuel salt (^{233}U , reactor-grade plutonium, TRU) at startup and at equilibrium (after ≈ 30 years of operation). Actinides evolution and poisonous fission product accumulation for various initial fissile compositions demonstrated the different effects on the SD-TMSR neutronics performance. For the Th/ ^{233}U , the thermal neutron flux is suppressed at the equilibrium because fissile ^{233}U in the core is being substituted with heavier fissile actinides: ^{235}U , ^{239}Pu , and ^{241}Pu . This is in good agreement with results in the literature [7, 25].

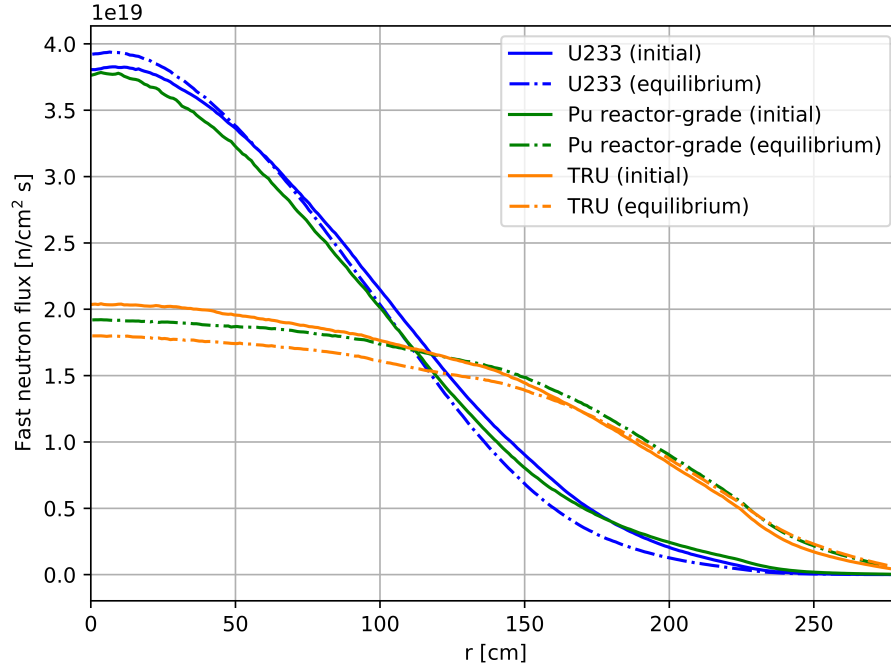


Figure 13: Radial fast neutron flux distribution for 3 different initial fuel salt compositions at startup and equilibrium (the fast flux confidence interval $\pm\sigma < 2.5\%$ for all cases).

Opposite behavior was observed for the Pu reactor-grade and TRU cases. For these cases, the thermal neutron flux is increasing during operation while

fast neutron flux is decreasing. Fissile plutonium nuclides (generate relatively hard spectrum) from initial fuel salt composition is gradually substituted with the ^{233}U (generates relatively soft spectrum), produced from the fertile ^{232}Th .
 325 During reactor operation, the ^{233}U becomes primary fissile isotope, which leads to the neutron spectrum softening of the reactor.

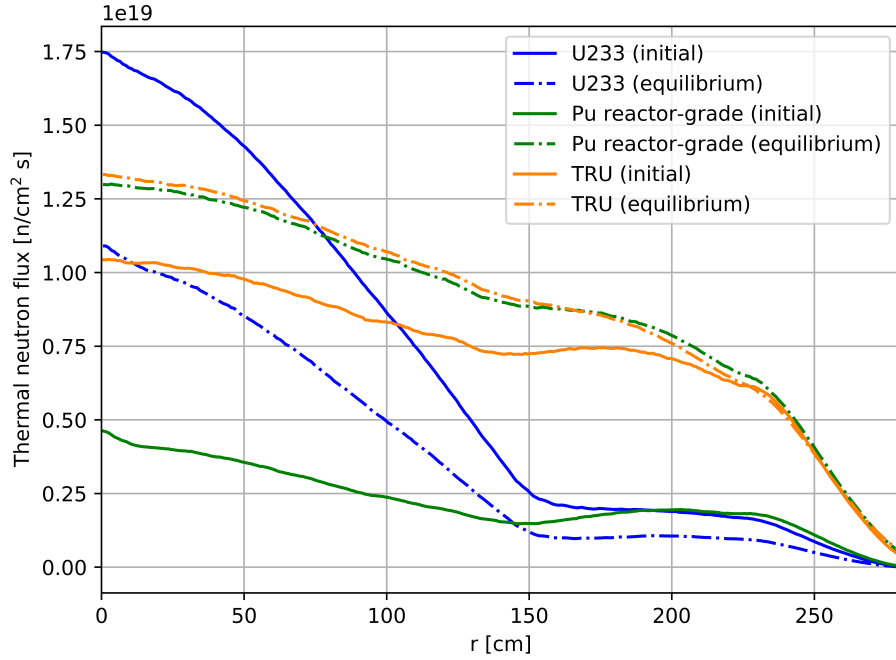


Figure 14: Radial thermal neutron flux distribution for 3 different initial fuel salt compositions at startup and equilibrium (the thermal flux confidence interval $\pm\sigma < 1.6\%$ for all cases).

Notably, more changes in thermal neutron flux shape and magnitude for ^{233}U case were observed in the inner core zone ($R \lesssim 150$) than in the outer core zone. In contrast, for Pu reactor-grade and TRU cases, significant changes were observed for thermal neutron flux in the outer core zone and reflector.
 330 Additionally, Figure 14 shows relatively large changes in thermal flux leakage from the core for the Pu and TRU cases. Overall, the SD-TMSR core design was optimized for ^{233}U fissile isotope [5]; thus, the core geometry (e.g., fuel channels lattice pitch) must be re-optimized for another type of fuel to obtain better

335 neutronics performance.

5.6. Temperature coefficient of reactivity

The temperature coefficient of reactivity quantifies reactivity changes due to temperature increase in the core and was calculated in this work as follows:

$$\alpha = \frac{k_{eff}(T_{i+1}) - k_{eff}(T_i)}{k_{eff}(T_{i+1})k_{eff}(T_i)(T_{i+1} - T_i)} \quad (2)$$

where

k_{eff} = effective multiplication factor

T_i = fuel salt temperature in (900 K, 1000 K).

Table 8 summarizes temperature coefficients calculated for three different initial fissile loads at the startup and at the equilibrium. By propagating the k_{eff} statistical error provided by SERPENT-2, uncertainty for each temperature coefficient was calculated using formula:

$$\delta\alpha = \left| \frac{1}{T_{i+1} - T_i} \right| \sqrt{\frac{\delta k_{eff}^2(T_{i+1})}{k_{eff}^4(T_{i+1})} + \frac{\delta k_{eff}^2(T_i)}{k_{eff}^4(T_i)}} \quad (3)$$

where

δk_{eff} = statistical error for k_{eff} from SERPENT-2 output.

Notably, other sources of uncertainty are neglected, such as cross-section measurement error and approximations inherent in the density dependence on temperature.

340 When the fuel salt temperature increases, the density of the salt decreases, but at the same time, the total volume of fuel salt in the core remains constant because it is bounded by the vessel. When the graphite temperature increases, the density of graphite decreases, creating additional space for the salt. The cross-section temperatures for the fuel and moderator were changed from 900
345 to 1000 K to determine the temperature coefficients. This work considered five different cases:

1. Fuel salt temperature (Doppler Effect) rising from 900 to 1000 K (first row in Table 8).
2. Fuel salt density decreasing from 3.3 to 3.233 g/cm³ (density change caused by temperature increase from 900 to 1000 K).
3. Total fuel salt temperature (Doppler+density) rising from 900 to 1000 K.
4. Graphite temperature (Doppler Effect) rising from 900 to 1000 K.
5. Whole reactor temperature rising from 900 K to 1000 K.

In the first case, the fuel temperature change only impacts cross-section temperature. In the second case, changes in the fuel temperature only impact density, and the third case takes into account both effects. The geometry for these three cases is unchanged because the fuel is a liquid. However, when the graphite blocks heat up, both the density and the geometry changing due to the thermal expansion of solid graphite. The graphite linear thermal expansion is not a dominating factor [5], and herein we focus only on Doppler Effect for the moderator temperature coefficient.

The Fuel Temperature Coefficient (FTC) is negative for all considered fuel compositions due to thermal Doppler broadening of the resonance capture cross-

Table 8: Temperature coefficients of reactivity for 3 different initial fuel salt compositions at startup and equilibrium. Confidence interval $\pm\sigma$ for all coefficients is between 0.11 and 0.16 pcm/K).

Reactivity coefficient (pcm/K)	Startup fissile material					
	²³³ U		Pu		TRU	
	Initial	Equil.	Initial	Equil.	Initial	Equil.
Fuel salt temperature	-4.96	-5.26	-4.99	-3.12	-3.23	-1.97
Fuel salt density	+1.49	+2.34	+1.54	-1.58	-0.37	-1.62
Total salt fuel	-3.77	-2.83	-3.22	-4.23	-3.25	-3.69
Graphite temperature	+1.45	+0.45	-2.68	-1.37	-1.44	-1.14
Total core	-1.77	-2.59	-6.54	-5.06	-4.79	-4.76

sections in the thorium. For ^{233}U case, the FTC decreases in magnitude by
 365 -25% due to neutron spectrum hardening during the reactor operation. For Pu
 reactor-grade and TRU cases, the FTC becomes more negative at the equilibrium,
 by $+31\%$ and $+14\%$, respectively. Spectrum softening for these fueling cases
 positively affects the FTC magnitude, and this effect seems to be proportional
 to the spectrum shift.

370 The Moderator Temperature Coefficient (MTC) for the ^{233}U case is positive
 and decreases during reactor operation because of spectrum hardening with
 fuel depletion. For other cases, the MTC is negative and also decreasing in
 magnitude during the reactor operation. Finally, the total temperature coefficient
 of reactivity is strongly negative for all considered scenarios but decreases in
 375 magnitude during reactor operation due to spectral shift. Notably, the total
 temperature coefficient is the most negative for the Pu reactor-grade case at
 startup, which has the hardest neutron spectrum (Figure 12). These coefficients
 agree with earlier estimates for SD-TMSR [5, 25] and MSBR [7, 32, 23].

Even after 30 years of operation, the total temperature coefficient of reac-
 380 tivity remains relatively large and negative (in the range between -2.59 and
 -5.06 pcm/K) comparing with the conventional PWR, which has temperature
 coefficient of about -1.71 pcm/ $^{\circ}\text{F} \approx -3.08$ pcm/K [33]), and allows excellent
 reactor stability and control. The additional analysis must be performed taking
 graphite moderator density change and linear thermal expansion into account,
 385 but material properties for the SD-TMSR graphite are not available in published
 literature. Alternatively, relatively well-studied reactor graphite (e.g., AXQ
 graphite [23]) can be considered as a candidate for the SD-TMSR concept.

5.7. Six Factor analysis

The effective multiplication factor can be expressed as follows:

$$k_{eff} = k_{inf} P_f P_t = \eta f p \epsilon P_f P_t \quad (4)$$

where

η = thermal fission factor

f = thermal utilization factor

p = resonance escape probability

ϵ = fast fission factor

P_f = fast non-leakage probability

P_t = thermal non-leakage probability.

Table 9 summarizes the six factors for 3 different initial fuel salt compositions at startup and equilibrium. By using SERPENT-2 built-in online reprocessing capabilities, all six factors have been calculated at the beginning of the operation and after 30 years of operation. Neutron population and number of active/inactive cycles were selected to obtain k_{eff} statistical uncertainty less than 12 pcm. The fast and thermal non-leakage probabilities remain constant regardless of initial fissile material and neutron spectrum shift during operation. The thermal utilization factor (f) remains almost constant during operation for ^{233}U and TRU cases but considerably declines for Pu case due to significant neutron spectrum softening.

Table 9: Six factors for the SD-TMSR model for 3 different initial fuel salt compositions at startup and equilibrium.

Factor	Startup fissile material					
	^{233}U		Pu		TRU	
	Initial	Equil	Initial	Equil	Initial	Equil
η	1.26	1.40	1.66	1.44	1.59	1.31
f	0.97	0.98	0.96	0.76	0.80	0.75
p	0.54	0.43	0.26	0.16	0.17	0.15
ϵ	1.49	1.67	2.45	5.87	4.83	6.81
P_f	0.99	0.99	0.99	0.99	0.99	0.99
P_t	1.00	1.00	1.00	1.00	1.00	1.00

In contrast, the neutron reproduction factor (η), resonance escape probability
400 (p), and fast fission factor (ϵ) differ notably between initial and equilibrium state
for all three initial fissile materials. The fast fission factor (ϵ) is much larger at
startup for Pu and TRU cases because these initial fissile materials provided a
much harder neutron spectrum than ^{233}U , and ϵ grows throughout the core's
lifetime. Conversely, the resonance escape probability decreases during reactor
405 operation. The thermal fission factor increases during reactor operation for the
 ^{233}U as initial fuel due to the accumulation of fissile plutonium isotopes, which
produce more neutrons per fission (ν). The other two scenarios demonstrated
opposite behavior: plutonium isotopes with large neutrons per fission production
(ν) are gradually substituted with the ^{233}U , which has lower ν [34]. This six
410 factors' evolution agrees with previously determined evolution parameters for a
similar single-fluid double-zone MSBR [25, 7, 35].

6. Conclusion

In the present paper, five different types of initial fissile materials have been
studied for transitioning to thorium fuel cycle in the SD-TMSR. The molar
415 composition of start-up fuel for all five cases is listed in Table 4, as well, the
inventories in Table 5. We adopted two different feed mechanisms; thorium feed
mechanism and non-thorium feed mechanism. The whole-core of the SD-TMSR
was simulated with Pu reactor-grade, TRU, and ^{233}U as initial fissile materials.
Additionally, the variation of the effective multiplication factor k_{eff} , inventory,
420 and other neutronic parameters have been investigated. Results demonstrated
that continuous flow of Pu reactor-grade helps in transition to thorium fuel
cycle within a relatively short time (≈ 4.5 years) compared to 26 years for
Th/ ^{233}U start-up fuel. Meanwhile, using TRU as initial fissile materials shows
the possibility of operating the SD-TMSR for a long period of time (≈ 40 years)
425 without any external feed of ^{233}U . In addition, the Pu proportion in fuel salt has
been calculated and found to be below the solubility limit. Finally, the neutron
spectrum shift during the reactor operation for the three selected cases has been

calculated.

7. Future work

430 8. Conflict of interest

The authors declare no conflict of interest.

9. Acknowledgments

Osama Ashraf would like to thank the Egyptian Ministry of Higher Education (MoHE), as well as MEPHI's Competitiveness Program for providing financial
435 support for this research. The facility and tools needed to conduct this work were supported by MEPHI.

The authors contributed to this work as described below.

Osama Ashraf conceived and designed the simulations, wrote the paper, prepared figures and/or tables, performed the computation work, and reviewed
440 drafts of the paper.

Andrei Rykhlevskii conceived and designed the simulations, wrote the paper, prepared figures and/or tables, performed the computation work, and reviewed drafts of the paper. Andrei Rykhlevskii is supported by DOE ARPA-E MEITNER program award DE-AR0000983.

445 G. V. Tikhomirov directed and supervised the work, conceived and designed the simulations and reviewed drafts of the paper. Prof. Tikhomirov is supported by Rosatom, he is Deputy Director of the Institute of Nuclear Physics and Engineering MEPHI. Board member of Nuclear society of Russia.

Kathryn D. Huff supervised the work, conceived and contributed to conception
450 of the simulations, and reviewed drafts of the paper. Prof. Huff is supported by the Nuclear Regulatory Commission Faculty Development Program, the National Center for Supercomputing Applications, the NNSA Office of Defense Nuclear Nonproliferation R&D through the Consortium for Verification Technologies and the Consortium for Nonproliferation Enabling Capabilities, the International

455 Institute for Carbon Neutral Energy Research (WPI-I2CNER), sponsored by
the Japanese Ministry of Education, Culture, Sports, Science and Technology,
and DOE ARPA-E MEITNER program award DE-AR0000983.

This research is part of the Blue Waters sustained-petascale computing
project, which is supported by the National Science Foundation (awards OCI-
460 0725070 and ACI-1238993) and the state of Illinois. Blue Waters is a joint effort
of the University of Illinois at Urbana-Champaign and its National Center for
Supercomputing Applications

References

- [1] DOE, US, A technology roadmap for generation iv nuclear energy systems
465 (2002) 48–52.
- [2] D. D. Siemer, Why the molten salt fast reactor (msfr) is the best gen iv
reactor, *Energy Science & Engineering* 3 (2) (2015) 83–97.
- [3] M. Rosenthal, P. Kasten, R. Briggs, Molten-salt reactorshistory, status, and
potential, *Nuclear Applications and Technology* 8 (2) (1970) 107–117.
- 470 [4] I. Pioro, Handbook of generation IV nuclear reactors, Woodhead Publishing,
2016.
- [5] G. C. Li, P. Cong, C. G. Yu, Y. Zou, J. Y. Sun, J. G. Chen, H. J. Xu,
Optimization of Th-U fuel breeding based on a single-fluid double-zone
thorium molten salt reactor, *Progress in Nuclear Energy* 108 (2018) 144–151.
475 doi:10.1016/j.pnucene.2018.04.017.
URL [http://www.sciencedirect.com/science/article/pii/
S0149197018300970](http://www.sciencedirect.com/science/article/pii/S0149197018300970)
- [6] A. Nuttin, D. Heuer, A. Billebaud, R. Brissot, C. Le Brun, E. Liatard,
J.-M. Loiseaux, L. Mathieu, O. Meplan, E. Merle-Lucotte, et al., Potential
480 of thorium molten salt reactorsdetailed calculations and concept evolution
with a view to large scale energy production, *Progress in nuclear energy*
46 (1) (2005) 77–99.

- [7] A. Rykhlevskii, J. W. Bae, K. D. Huff, Modeling and simulation of online reprocessing in the thorium-fueled molten salt breeder reactor, *Annals of Nuclear Energy* 128 (2019) 366–379. doi:10.1016/j.anucene.2019.01.030.
- [8] E. Merle-Lucotte, D. Heuer, C. Le Brun, J. Loiseaux, Scenarios for a worldwide deployment of nuclear energy production.
- [9] B. R. Betzler, J. J. Powers, A. Worrall, Modeling and simulation of the start-up of a thorium-based molten salt reactor, in: *Proc. Int. Conf. PHYSOR*, 2016.
- [10] C. Zou, C. Cai, C. Yu, J. Wu, J. Chen, Transition to thorium fuel cycle for tmsr, *Nuclear Engineering and Design* 330 (2018) 420–428.
- [11] C. Zou, G. Zhu, C. Yu, Y. Zou, J. Chen, Preliminary study on trus utilization in a small modular th-based molten salt reactor (smtmsr), *Nuclear Engineering and Design* 339 (2018) 75–82.
- [12] D. Heuer, E. Merle-Lucotte, M. Allibert, M. Brovchenko, V. Ghetta, P. Rubiolo, Towards the thorium fuel cycle with molten salt fast reactors, *Annals of Nuclear Energy* 64 (2014) 421–429.
- [13] O. Ashraf, A. Smirnov, G. Tikhomirov, Modeling and criticality calculation of the molten salt fast reactor using serpent code, in: *Journal of Physics: Conference Series*, Vol. 1189, IOP Publishing, 2019, p. 012007.
- [14] O. Ashraf, A. Smirnov, G. Tikhomirov, Nuclear fuel optimization for molten salt fast reactor, in: *Journal of Physics: Conference Series*, Vol. 1133, IOP Publishing, 2018, p. 012026. doi:10.1088/1742-6596/1133/1/012026.
- [15] C. Fiorina, M. Aufiero, A. Cammi, F. Franceschini, J. Krepel, L. Luzzi, K. Mikityuk, M. E. Ricotti, Investigation of the msfr core physics and fuel cycle characteristics, *Progress in Nuclear Energy* 68 (2013) 153–168.

- 510 [16] C. de Saint Jean, M. Delpech, J. Tommasi, G. Youinou, P. Bourdot,
Scénarios cne: réacteurs classiques, caractérisation à l'équilibre, rapport
CEA DER/SPRC/LEDC/99-448.
- [17] A. Rykhlevskii, B. R. Betzler, A. Worrall, K. D. Huff, Fuel Cycle Perfor-
mance of Fast Spectrum Molten Salt Reactor Designs, in: Proceedings of
515 Mathematics and Computation 2019, American Nuclear Society, Portland,
OR, 2019.
- [18] B. R. Betzler, A. Rykhlevskii, A. Worrall, K. Huff, Impacts of Fast-Spectrum
Molten Salt Reactor Characteristics on Fuel Cycle Performance, Tech. rep.,
Oak Ridge National Lab.(ORNL), Oak Ridge, TN (United States) (2019).
- 520 [19] J. Leppänen, M. Pusa, T. Viitanen, V. Valtavirta, T. Kaltiaisenaho, The
serpent monte carlo code: Status, development and applications in 2013,
in: SNA+ MC 2013-Joint International Conference on Supercomputing in
Nuclear Applications+ Monte Carlo, EDP Sciences, 2014, p. 06021.
- [20] M. Jiang, H. Xu, Z. Dai, Advanced fission energy program-tmsr nuclear
525 energy system, Bull. Chin. Acad. Sci 27 (3) (2012) 366–374.
- [21] X. Li, X. Cai, D. Jiang, Y. Ma, J. Huang, C. Zou, C. Yu, J. Han, J. Chen,
Analysis of thorium and uranium based nuclear fuel options in fluoride
salt-cooled high-temperature reactor, Progress in Nuclear Energy 78 (2015)
285–290.
- 530 [22] G. Li, Y. Zou, C. Yu, et al., Model optimization and analysis of th-u
breeding based on msfr, Nucl. Tech 40 (2017) 020603–020603.
- [23] R. C. Robertson, Conceptual Design Study of a Single-Fluid Molten-Salt
Breeder Reactor., Tech. Rep. ORNL-4541, comp.; Oak Ridge National
Laboratory, Tenn. (Jan. 1971).
535 URL <http://www.osti.gov/scitech/biblio/4030941>
- [24] J. C. Marka, Explosive properties of reactor-grade plutonium, Science &
Global Security 4 (1) (1993) 111–128.

- [25] O. Ashraf, A. Rykhlevskii, G. Tikhomirov, K. D. Huff, Whole core analysis of the single-fluid double-zone thorium molten salt reactor (sd-tmsr), *Annals of Nuclear Energy*.
540
- [26] N. OECD, Probabilistic safety assessment in nuclear power plant management: a report by a group of experts of the nea committee on the safety of nuclear installations, june 1989, 112 (1989).
- [27] J. Serp, M. Allibert, O. Beneš, S. Delpech, O. Feynberg, V. Ghetta, D. Heuer, D. Holcomb, V. Ignatiev, J. L. Kloosterman, et al., The molten salt reactor (msr) in generation iv: overview and perspectives, *Progress in Nuclear Energy* 77 (2014) 308–319.
545
- [28] M. Aufiero, A. Cammi, C. Fiorina, J. Leppänen, L. Luzzi, M. E. Ricotti, An extended version of the serpent-2 code to investigate fuel burn-up and core material evolution of the molten salt fast reactor, *Journal of Nuclear Materials* 441 (1-3) (2013) 473–486.
550
- [29] A. Isotalo, M. Pusa, Improving the accuracy of the chebyshev rational approximation method using substeps, *Nuclear Science and Engineering* 183 (1) (2016) 65–77.
- [30] V. Ignatiev, O. Feynberg, A. Merzlyakov, A. Surenkov, A. Zagnitko, V. Afonichkin, A. Bovet, V. Khokhlov, V. Subbotin, R. Fazilov, et al., Progress in development of mosart concept with th support, in: *Proceedings of ICAPP*, Vol. 12394, 2012.
555
- [31] D. Sood, P. Iyer, R. Prasad, V. Vaidya, K. Roy, V. Venugopal, Z. Singh, M. Ramaniah, Plutonium trifluoride as a fuel for molten salt reactors-solubility studies, *Nuclear technology* 27 (3) (1975) 411–415.
560
- [32] A. Rykhlevskii, A. Lindsay, K. D. Huff, Full-core analysis of thorium-fueled Molten Salt Breeder Reactor using the SERPENT 2 Monte Carlo code, in: *Transactions of the American Nuclear Society*, American Nuclear Society, Washington, DC, United States, 2017.
565

- [33] B. Forget, K. Smith, S. Kumar, M. Rathbun, J. Liang, Integral Full Core Multi-Physics PWR Benchmark with Measured Data, Tech. rep., Massachusetts Institute of Technology (2018).
- [34] N. G. Sjöstrand, J. S. Story, Cross sections and neutron yields for U-233, U-235 and Pu-239 at 2200 m/sec, Tech. rep., AB Atomenergi (1960).
570
- [35] J. Park, Y. Jeong, H. C. Lee, D. Lee, Whole core analysis of molten salt breeder reactor with online fuel reprocessing, International Journal of Energy Research 39 (12) (2015) 1673–1680. doi:10.1002/er.3371.
URL <http://doi.wiley.com/10.1002/er.3371>